

Large Torque Variations in Two Soft Gamma Repeaters

Peter M. Woods^{1,2}, Chryssa Kouveliotou^{2,3}, Ersin Göğüş^{2,4}, Mark H. Finger^{1,2}, Jean Swank⁵,
Craig B. Markwardt⁵, Kevin Hurley⁶ and Michiel van der Klis⁷

ABSTRACT

We have monitored the pulse frequencies of the two soft gamma repeaters SGR 1806–20 and SGR 1900+14 through the beginning of year 2001 using primarily *Rossi X-ray Timing Explorer* Proportional Counter Array observations. In both sources, we observe large changes in the spin-down torque up to a factor of ~ 4 , which persist for several months. Using long baseline phase-connected timing solutions as well as the overall frequency histories, we construct torque noise power spectra for each SGR. The power spectrum of each source is very red (power-law slope ~ -3.5). The torque noise power levels are consistent with some accreting systems on time scales of ~ 1 year, yet the full power spectrum is much steeper in frequency than any known accreting source. To the best of our knowledge, torque noise power spectra with a comparably steep frequency dependence have only been seen in young, glitching radio pulsars (e.g. Vela). The observed changes in spin-down rate do not correlate with burst activity, therefore, the physical mechanisms behind each phenomenon are also likely unrelated. Within the context of the magnetar model, seismic activity cannot account for both the bursts and the long-term torque changes unless the seismically active regions are decoupled from one another.

Subject headings: stars: individual (SGR 1900+14) — stars: individual (SGR 1806-20)
— stars: pulsars — X-rays: bursts

¹Universities Space Research Association; peter.woods@msfc.nasa.gov

²National Space Science and Technology Center, 320 Sparkman Dr. Huntsville, AL 35805

³NASA Marshall Space Flight Center

⁴Department of Physics, University of Alabama in Huntsville, Huntsville, AL 35899

⁵NASA Goddard Space Flight Center, Greenbelt, MD 20771

⁶University of California at Berkeley, Space Sciences Laboratory, Berkeley, CA 94720-7450

⁷Astronomical Institute “Anton Pannekoek” and CHEAF, University of Amsterdam, 403 Kruislaan, 1098 SJ Amsterdam, NL

1. Introduction

Shortly after the first radio pulsars were discovered in 1967 (Hewish et al. 1968), it was found that the pulse frequency of the Crab (one of the early pulsars) was decreasing steadily with time (Richards & Comella 1969). This behavior matched very nicely with that expected of an isolated, magnetized neutron star spinning down via magnetic braking (Pacini 1967; Gold 1968). Since then, precise, long-term monitoring of radio pulsars has shown the presence of timing irregularities in most if not all sources. In isolated pulsars, these deviations can be grouped into two broad categories: (i) glitches or discontinuous increases in the spin frequency (Radhakrishnan & Manchester 1969; Reichley & Downs 1969) and (ii) timing noise which can be described as a more gradual drifting of the *measured* torque on the star (Boynton et al. 1972).

In the last few years, a small group of isolated X-ray pulsars has been identified with timing properties qualitatively similar to, but more extreme than those of radio pulsars. This group comprises nine sources, four of which are known as Soft Gamma Repeaters (SGRs) and five as Anomalous X-ray Pulsars (AXPs). Like radio pulsars, these sources are spinning down and show timing noise, however, at magnitudes on average one hundred times larger. Interpreted as magnetic braking, their very rapid spin-down would suggest SGRs/AXPs have magnetic fields in the $10^{14} - 10^{15}$ G range (Thompson & Duncan 1996; Kouveliotou et al. 1998, 1999).

Collectively, the SGRs and AXPs possess persistent luminosities of order $\sim 10^{34} - 10^{35}$ ergs s^{-1} , soft X-ray spectra (as compared to accreting systems), spin periods within a narrow range (5–12 s), rapid spin-down rates (frequency derivatives $\sim 10^{-12}$ Hz s^{-1}), and strong timing noise (see Hurley 2000 and Mereghetti 2000 for recent reviews on SGRs and AXPs, respectively). The primary difference between AXPs and SGRs is that so far, only SGRs have been observed to burst. SGR bursts often occur in bunches, with active periods lasting on average a few weeks, recurring at time intervals of years (e.g. Göğüş et al. 2001). Occasionally, they emit extremely long and bright bursts, now known as “giant flares”. Only two such flares have been recorded so far: one from SGR 0526–66 on March 5, 1979 (Mazets et al. 1979) and more recently one from SGR 1900+14 on August 27, 1998 (Hurley et al. 1999a; Feroci et al. 1999, 2001; Mazets et al. 1999). In each of these flares, a hard, bright initial spike (peak luminosity $\sim 10^{44}$ ergs s^{-1}) was followed by a slowly decaying, several minute long tail showing coherent pulsations at periods of 8 and 5 s, respectively. In fact, the existence of strongly magnetized neutron stars or ‘magnetars’ (Duncan & Thompson 1992) in SGRs was first proposed based primarily upon the first of these giant flares from SGR 0526–66 (Duncan & Thompson 1992; Paczyński 1992; Thompson & Duncan 1995).

In the magnetar model, it is the decay of the strong magnetic field which powers both the persistent and burst emissions (Thompson & Duncan 1995, 1996). The short duration SGR bursts are believed to be triggered by starquakes induced by magnetic stresses in the neutron star crust. Cracking the crust leads to a sudden injection of Alfvén waves into the magnetosphere, particle acceleration, and ultimately, the formation of an optically thick pair plasma which cools and

radiates. The giant flares involve a more profound restructuring of the crust and magnetic field on a global scale (Thompson & Duncan 1995; Woods et al. 2001; Ioka 2001). The persistent X-ray emission from magnetars is believed to be due to persistent magnetospheric currents driven by twists in the evolving magnetic field (Thompson & Duncan 1996), thermal emission from the stellar surface (e.g. Özel 2001) heated by the decay of the strong field (Thompson & Duncan 1996), or some combination of the two. In any hybrid model, however, the pulse fraction of each spectral component must be nearly the same in order to account for the weak or absent energy dependence of the pulse fraction in these sources (Özel, Psaltis & Kaspi 2001). The rapid spindown of the neutron star is believed to be due to magnetic dipole radiation in combination with a wind of relativistic particles, qualitatively similar to radio pulsars.

Alternatives to the magnetar model for SGRs and AXPs invoke accretion to explain their persistent X-ray luminosities. In this scenario, accretion torques act upon a neutron star with a ‘standard’ field strength ($\sim 10^{12}$ G) spinning it down rapidly. In line with the strict constraints on binary companions accompanying the SGRs and AXPs (e.g. Mereghetti, Israel & Stella 1998; Wilson et al. 1999; Woods et al. 2000; Patel et al. 2001), the neutron star is still isolated, yet retains a fallback disk left over from the supernova explosion that formed the neutron star. These models naturally explain the narrow period distribution and can account for the relatively strong torque variability in general. However, these models fail to adequately explain the super-Eddington bursts in the case of SGRs. Furthermore, for some AXPs (e.g. Hulleman, van Kerkwijk & Kulkarni 2000; Hulleman et al. 2000) and SGR 0526–66 (Kaplan et al. 2001), the observed brightness levels and in some cases upper limits of optical/IR counterparts are well below what is expected from reprocessed X-ray emission within a disk. Finally, the detection of optical pulsations at high rms from 4U 0142+61 (Kern & Martin 2001) are implausible in the context of this model.

Here, we report on our long-term X-ray observations of SGR 1806–20 and SGR 1900+14 using predominantly data from the *RXTE* PCA. We show that each SGR undergoes an extended ($\gtrsim 1$ year) interval of accelerated spin-down where the measured torque on the star increases by a factor ~ 4 . We directly compare the burst activity of each source with the long-term torque variability. The timing noise is quantified in two ways. We measure the timing noise parameter Δ and also construct torque noise power spectra for each source. The timing noise measurements for these SGRs are compared with the measured noise strengths in known accreting systems and radio pulsars. Finally, we discuss implications these results have on the models for torque variability in magnetars, and what constraints they impose upon SGR models in general.

2. SGR 1900+14

Shortly after the discovery of pulsations from SGR 1900+14 in 1998 (Hurley et al. 1999b), it was realized that the source did not have a constant spin-down rate (Kouveliotou et al. 1999). Using archival data, it was determined that the *average* spin-down rate between 1996 September and 1998 June was $\sim -2.3 \times 10^{-12}$ Hz s $^{-1}$ (Marsden et al. 1999; Woods et al. 1999a), however,

the local rate in 1996 September (far removed from burst activity) was significantly higher, at $-3.1 \times 10^{-12} \text{ Hz s}^{-1}$ (Woods et al. 1999b).

The SGR became active again in May 1998 and burst for almost one year, during which a giant flare was observed on 1998 August 27 (Hurley et al. 1999a; Mazets et al. 1999; Feroci et al. 1999, 2001). Between 1998 June and the day following the giant flare, the average spin-down rate doubled. Due to the absence of frequency measurements during this time interval, it was not known whether this accelerated spin-down was gradual, spanning the gap in observations, or was instead a sudden jump, perhaps linked with the giant flare (Woods et al. 1999b; Thompson et al. 2000). Recently, Palmer (2001) has shown that the phase of the pulsations during the tail of the flare does not match that expected from an extrapolation of the ephemeris determined shortly following the flare (~ 1 day). Assuming that there is no strong energy dependence in the pulse profile, this suggests that the star underwent a very rapid spin-down ($\dot{\nu} \sim -6 \times 10^{-10} \text{ Hz s}^{-1}$) during the hours following the August 27th flare. This result provides independent evidence for a transient particle wind blown off the surface during the flare (Frail, Kulkarni & Bloom 1999; Thompson et al. 2000) and eliminates the need for a “braking” glitch at the time of the flare. From 1998 August 28 through 1998 October 8, during a very intensive burst active interval, the spin-down rate was constant at $-2.23(1) \times 10^{-12} \text{ Hz s}^{-1}$, which is the least rapid spin-down rate observed to date for this source. In the following, we present our analysis of X-ray data starting in 1999 January and continuing through 2001 January. During these two years, we measure the largest spin-down rates yet seen from this SGR.

Our first set of observations was obtained with the *RXTE* PCA from 1999 January through 1999 July. Partial results from these data were reported in Woods et al. (1999b). Here, we have analyzed the full data set. The sequence of *RXTE* pointings at SGR 1900+14 began with a long (~ 50 ks) observation and was followed by 26 shorter (~ 10 ks) observations whose spacing grew from 0.5 days to ~ 8 days. The observations were structured in this manner in order to enable us to phase connect the data (count cycles) and thereby track the pulse frequency across the full extent of the data set. We successfully connected the early observations covering the first 14 days beginning on MJD 51181 (1999 January 3). Even during this short span of data, we were detecting curvature in the phases (i.e. spin down). The next observation took place eight days later on MJD 51203 (1999 January 25); the measured phase was inconsistent with an extrapolation of our model. We checked to see whether the inconsistency was due to a change in the pulse profile during the eight day gap in observations, however, there was no measureable change. Unfortunately, we were not able to phase connect the remainder of the data.

In an attempt to recover the pulse phase ephemeris during this epoch, we constructed Lomb-Scargle power spectra (Lomb 1976) for each observation. These power spectra were converted to frequencies and combined into a grayscale plot to form a dynamic power spectrum (Figure 1) which clearly shows the spin-down trend of the SGR. We used these power spectra to perform a grid search in frequency and frequency derivative space. Choosing MJD 51280 as our epoch we searched frequencies from 0.19357 Hz to 0.19387 Hz and frequency derivatives

from $-20.0 \times 10^{-12} \text{ Hz s}^{-1}$ to $+6.7 \times 10^{-12} \text{ Hz s}^{-1}$. We assign the power in each grid point by averaging the intersections of the various power spectra with the simple model (i.e. frequency and frequency derivative). We show a contour map of the power in this grid in Figure 2. The frequency (0.193732 Hz) and frequency derivative ($-3.6 \times 10^{-12} \text{ Hz s}^{-1}$) corresponding to the peak power in this grid is overplotted in Figure 1 as a dashed line.

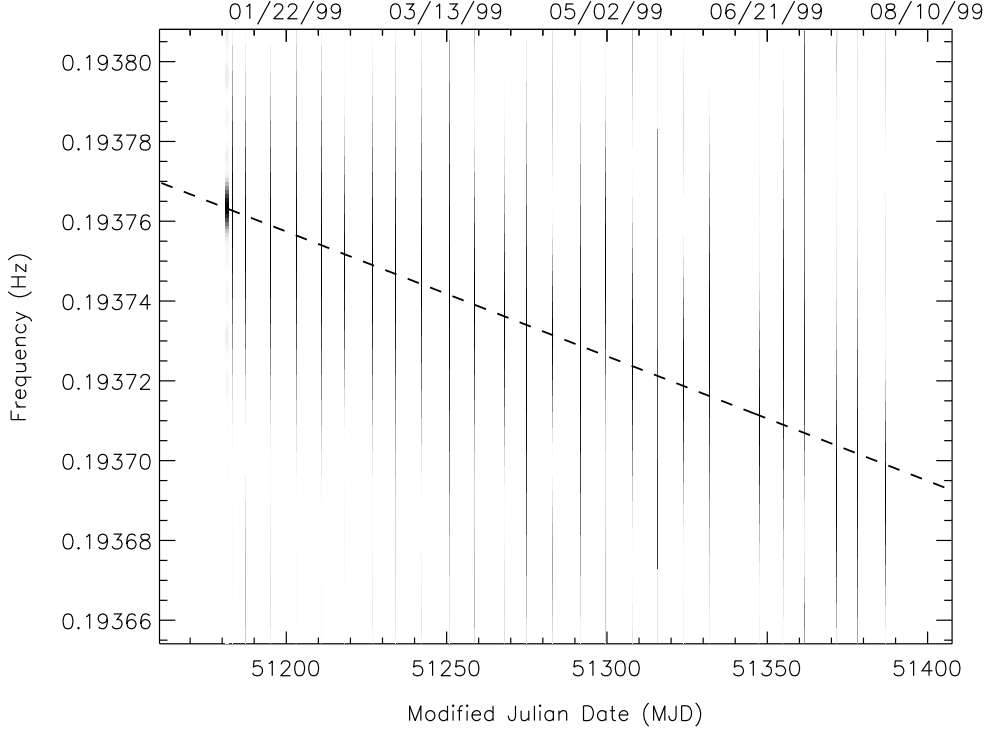


Fig. 1.— Dynamic Lomb-Scargle power spectrum of SGR 1900+14 during the first half of 1999. Darker regions denote higher power. The dashed line marks the average ephemeris as determined from a grid search of this power spectrum in frequency and frequency derivative space (see Fig 2).

Using the rough ephemeris found through the grid search described above, we folded all the data after the gap where we lost track of the phases. Unfortunately, we still could not construct a reliable phase connected solution for these data despite finding no significant changes in the pulse profile. Consequently, we are limited to coarse, independent frequency measurements from the Lomb-Scargle power spectra and a rough ephemeris for the full range of data provided by the grid search. The individual frequencies for each observation are listed in Table 1.

To constrain the manner in which the torque changed early within our observing campaign, we tried fitting a glitch phase model to the data near the time of the change allowing for either a positive (ordinary glitch) or negative (braking glitch) jump in frequency. We find that neither glitch model provides a significantly better fit to both the phase and frequency data over a higher

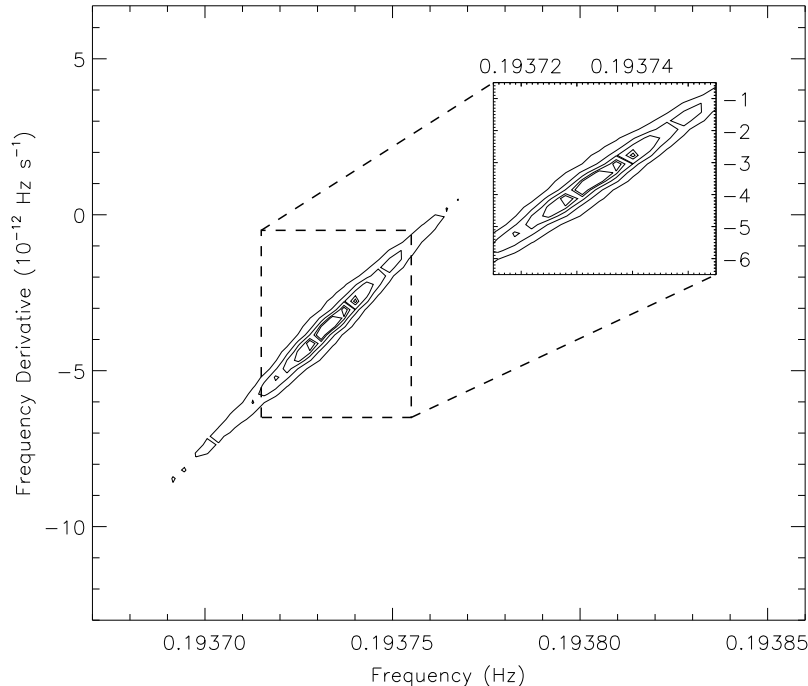


Fig. 2.— Contour map of average Lomb power for a grid search to the SGR 1900+14 data shown in Figure 1 (see text for details).

order polynomial with an equal number of free parameters. Furthermore, extrapolating the post-glitch ephemerides does not provide an adequate fit to the data during the following several weeks. Therefore, we conclude that the observed drifting in phase of the SGR 1900+14 pulsations during 1999 is not due to a simple shift in frequency and frequency derivative (i.e. a glitch). Instead, these data suggest strong timing noise in SGR 1900+14 on a short timescale ($\lesssim 1$ week).

The next set of observations of SGR 1900+14 took place in 2000 March and April with the BeppoSAX NFI. The spectral results have been reported in Woods et al. (2001). Here, we present the timing results from these data. For each observation, we extracted counts from the combined MECS images from a $4'$ radius circle centered on the source and barycenter corrected the photon arrival times. We then constructed a Lomb-Scargle power spectrum across a narrow range of frequencies (0.192 – 0.194 Hz). In each observation, we find a significant peak ($\gtrsim 5\sigma$) that we attribute to the spin frequency of the neutron star. We then split each observation into ~ 12 sections and refined our frequency measurement by fitting a line to the relative phases of each section. The spin frequency measurements are listed in Table 1. We find that the frequency derivative between 2000 March and April exceeds the average value observed during both the quiescent interval prior to burst activity and the most burst active interval (1998 September) by a factor ~ 4 .

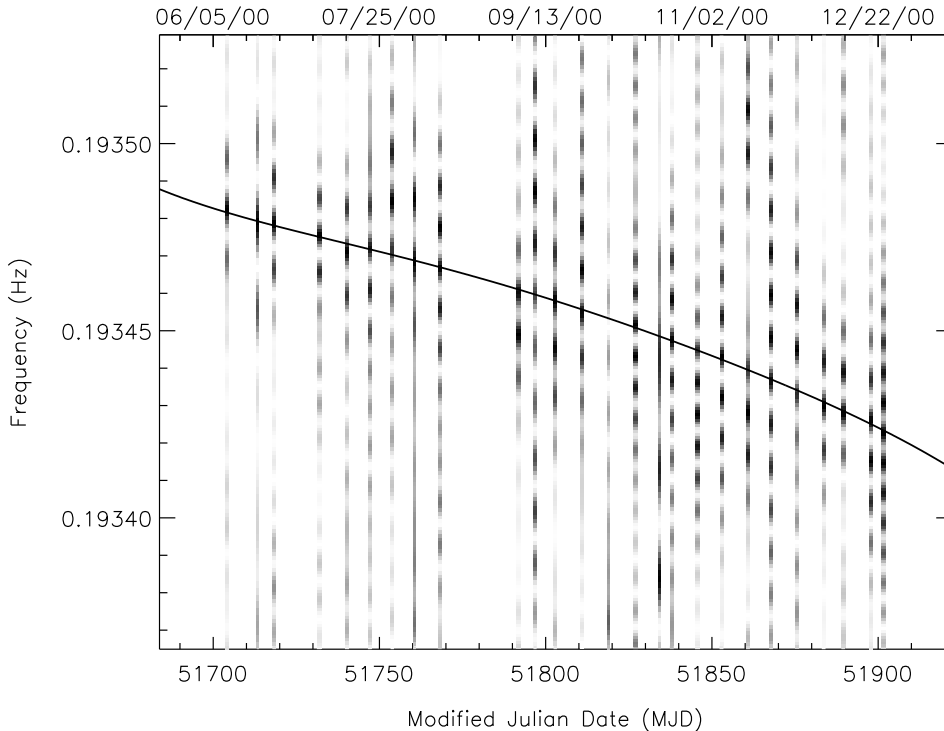


Fig. 3.— Dynamic Lomb-Scargle power spectrum of SGR 1900+14 during 2000. Darker regions denote higher power. The solid line marks the phase-connected timing solution to these data.

We began a long-term monitoring campaign of SGR 1900+14 with the *RXTE* PCA early in 2000. These observations continued with only minimal interruption through 2001 January. Initially, the schedule was structured as before with a single observation for each week. In 2000 June, the observing schedule was greatly improved by splitting the observations into pairs of ~ 10 ks exposure each separated by several spacecraft orbits. Extending the temporal baseline of the observations smears out the pulsed signal, but increases the frequency resolution. As with the PCA data from 1999, we constructed a dynamic Lomb-Scargle power spectrum (Figure 3). The frequency resolution (i.e. band separation in Figure 3) varies with changes in the spacing of each pair of observations. This enabled us to better track the pulse frequency through the observations and to phase connect the entire data set. The phase residuals are shown in Figure 4 after subtraction of a second order polynomial (*top*) and a sixth order polynomial (*bottom*). The residuals found after removing the sixth order polynomial are consistent with the measurement uncertainties ($\chi^2 = 23.3$ for 20 dof). The best fit ephemeris is reported in Table 2 and overplotted on Figure 3 (solid line). Within this 210 day stretch of data the frequency derivative changes by nearly a factor of 2, but the pulsed flux is consistent with remaining constant.

We have combined the timing results presented here with previous frequency measurements

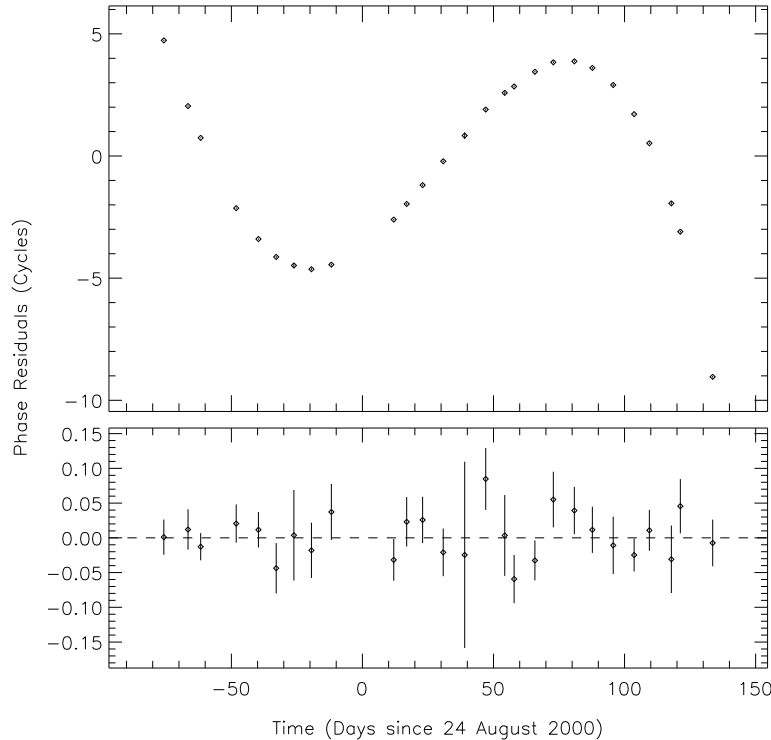


Fig. 4.— Phase residuals for SGR 1900+14 during year 2000 minus a quadratic trend (*top*) and minus a 6th order polynomial (*bottom*).

in order to construct a frequency history of SGR 1900+14 (Figure 5). The plotting symbols mark individual frequency measurements and the solid lines denote phase-connected timing solutions. Note that some line segments are too short to be seen on this scale. Throughout the 4.3 year frequency history of SGR 1900+14, we find no evidence for episodes of spin-up. We note that the overall coverage of observations is fairly sparse, so small amplitude short-term spin-up episodes cannot be excluded. The dashed line is the average spin-down rate measured prior to burst activation of the source in 1998. Extrapolation of this early trend in the spin-down clearly shows the large changes in torque imparted upon SGR 1900+14.

Plotted above the frequency history is the burst rate history of SGR 1900+14 (Woods et al. 1999b) as observed with the Burst and Transient Source Experiment (BATSE) onboard the *Compton Gamma-ray Observatory* (*CGRO*). The hashed region starting in 2000 June marks the end of the source monitoring with BATSE after the demise of *CGRO*. It is clear from this figure that the periods of enhanced torque do not correlate directly with the burst activity, confirming earlier results (Woods et al. 1999b). However, one cannot rule out a causal relationship between the two with a delay of several months between the burst activity and the subsequent torque variability. Unfortunately, the limited coverage of the persistent X-ray source during the last 20 years does not allow concrete conclusions on this relationship (see also §5).

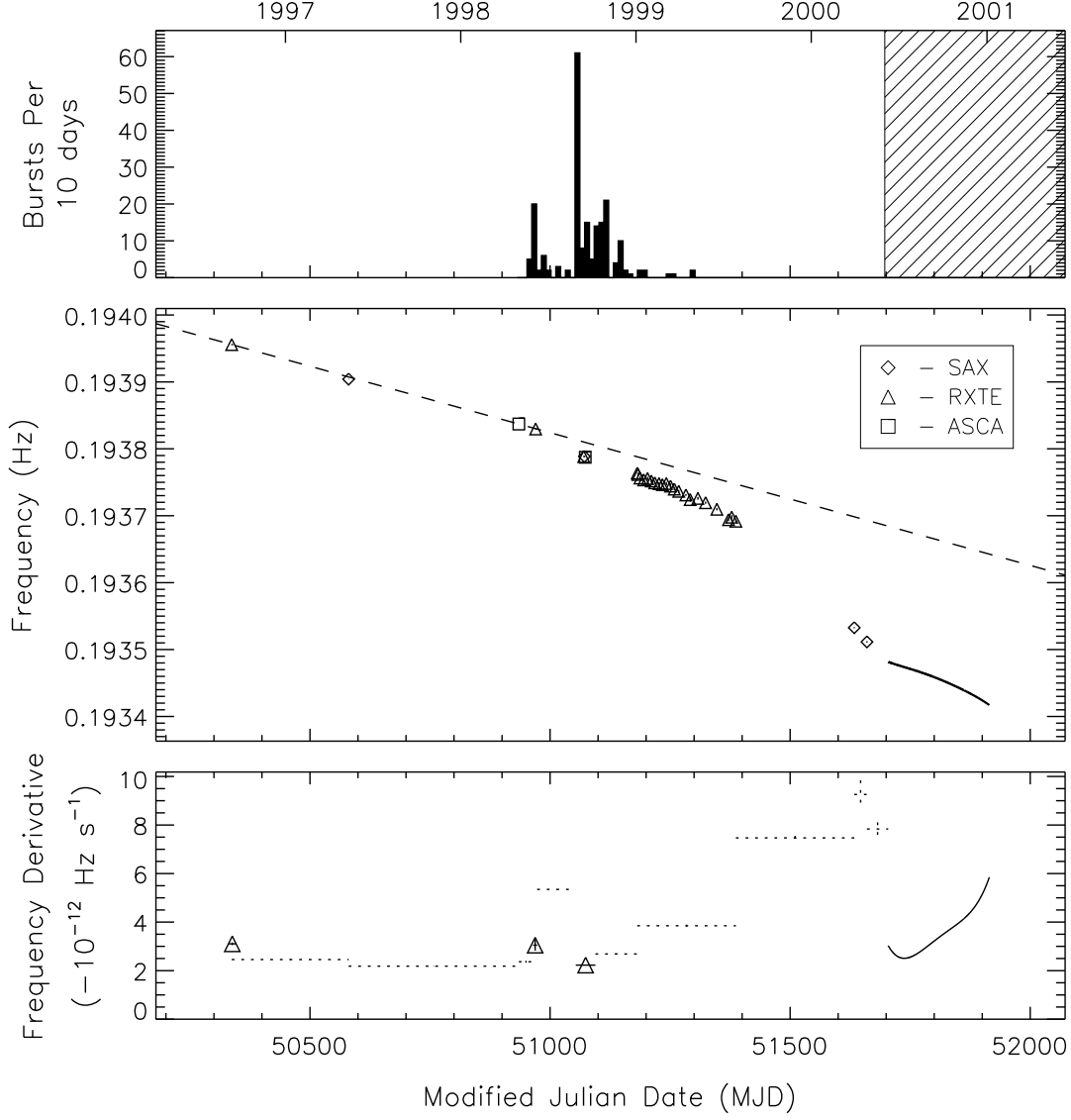


Fig. 5.— *Top* – Burst rate history of SGR 1900+14 as observed with BATSE. The hashed region starts at the end of the *CGRO* mission. *Middle* – The frequency history of SGR 1900+14 covering 4.3 years. Plotting symbols mark individual frequency measurements and solid lines denote phase-connected timing solutions. The dashed line marks the average spin-down rate prior to burst activation in 1998. *Bottom* – The frequency derivative history over the same timespan. Dotted lines denote average frequency derivative levels between widely spaced frequency measurements. Solid lines mark phase-coherent timing solutions and triangles mark instantaneous torque measurements, both using *RXTE* PCA data.

3. SGR 1806–20

From 1993 through 1998, there were only three X-ray observations of SGR 1806–20. Using these observations, Kouveliotou et al. (1998) determined that the SGR had an average spin-down rate of $-1.5 \times 10^{-12} \text{ Hz s}^{-1}$ over this time interval. Early in 1999, we initiated a sequence of PCA observations of this SGR which lasted for 178 days. The data were successfully phase connected and although the long-term frequency derivative did not change by very much, significant short-term deviations (timescale of months) were found (Woods et al. 2000). To model these deviations, we fit a constant spin-down plus an orbit to all available phases and frequencies between 1993 and 1999; the fit was statistically acceptable. Given the sparseness of the data, however, it was not possible to determine whether the observed torque variations were due to orbital effects or strong timing noise. We have recently completed the analysis of new *RXTE* PCA observations during year 2000 (January through November) to address this question.

Early in January 2000, SGR 1806–20 entered a moderately burst active state that led us to initiate densely sampled ToO observations with the PCA. The initial observation contained two notable surprises. First, the measured frequency (Table 3) was substantially smaller than expected based upon an extrapolation of the historical frequency history, effectively ruling out previously acceptable orbital solutions (Woods et al. 2000). In addition, the phase residuals (Figure 6) were

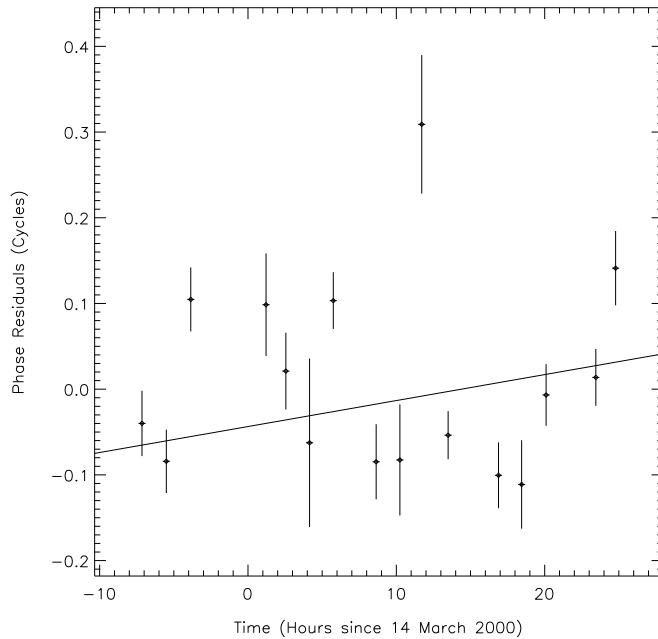


Fig. 6.— Phases for SGR 1806–20 during a long observation in March 2000. The solid line denotes a least-squares fit to the data.

unusually large ($\chi^2 = 73.1$ for 14 dof) for such a relatively short stretch of data (1.3 days). The pulse profile appears sinusoidal during these observations showing no gross changes throughout. This is the shortest timescale (\sim hours) over which we have observed timing noise in SGR 1806–20 thus far. We note, however, that SGR 1900+14 displayed timing noise on an even shorter timescale (\sim minutes) during *Chandra* observations following a recent burst activation of this source in 2001 (Kouveliotou et al. 2001).

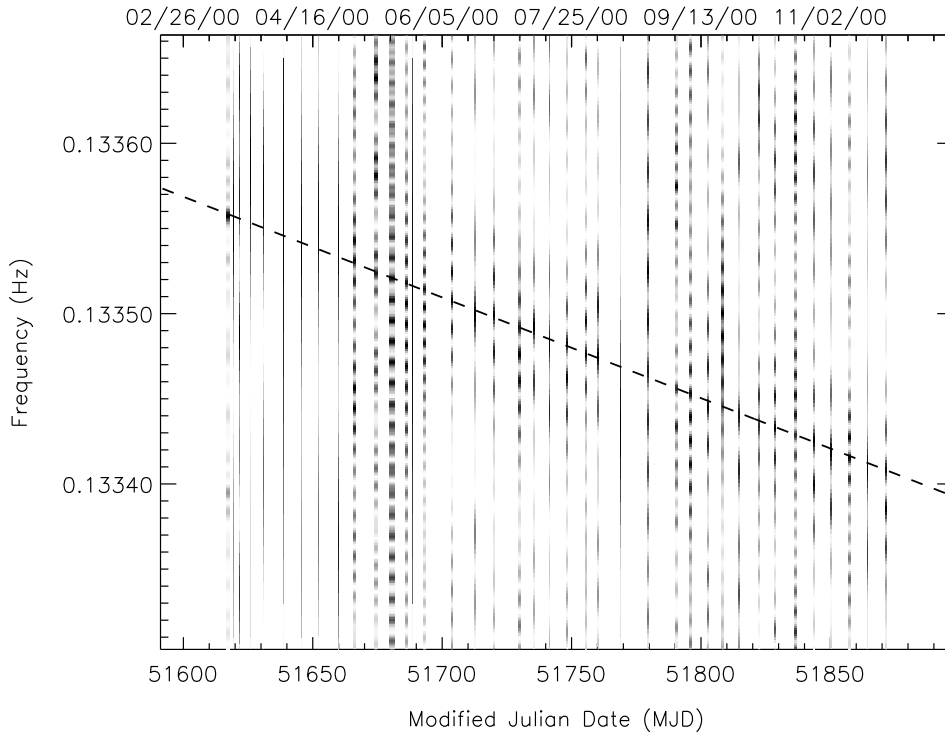


Fig. 7.— Dynamic Lomb-Scargle power spectrum of SGR 1806–20 during the year 2000. Darker regions denote higher power. The dashed line marks the average ephemeris as determined from a grid search of this power spectrum in frequency and frequency derivative space (see Figure 8).

After this initial observation, we began brief (~ 5 ks) weekly observations of the source. The torque variations continued, negating the possibility of achieving long baseline phase coherent solutions. In 2000 May, the weekly observation schedule was restructured employing the same strategy as was done for SGR 1900+14. For SGR 1806–20, exposure time of each pointing was ~ 5 ks with a total of 10 ks per pair per week. Observations of SGR 1806–20 continued until the source was no longer observable by *RXTE* due to Sun angle constraints in November. We next constructed a dynamic Lomb-Scargle power spectrum using these data (Figure 7) and performed a grid search in frequency (0.13340 to 0.13355 Hz) and frequency derivative (-20.0 to $+6.7 \times 10^{-12}$ Hz s $^{-1}$) space. The Lomb-Scargle power map (Figure 8) reaches a maximum at 0.1334800 Hz and

$-6.85 \times 10^{-12} \text{ Hz s}^{-1}$ for the frequency and frequency derivative, respectively. The epoch chosen for the grid search was MJD 51750. This best fit average ephemeris is overplotted in Figure 7.

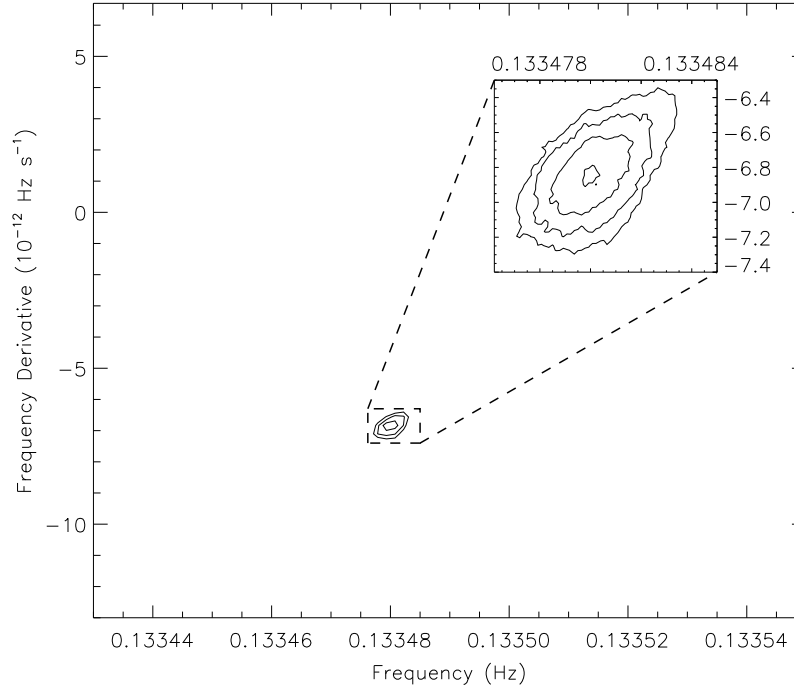


Fig. 8.— Contour map of average Lomb power for a grid search to the SGR 1806–20 data shown in Figure 7 (see text for details).

We find that the spin-down rate during the year 2000 is a factor ~ 4 larger than the average rate between 1993 and 1999. Unlike SGR 1900+14, we were not able to phase connect across the full extent of these data. However, we were able to connect a 55 day subset between MJD 51666 and 51720 (Table 4). For a 77 day subset between MJD 51796 and 51872, we attained a formally acceptable fit to the phases and frequencies. However, we are not fully confident that there are no cycle count ambiguities in this span of data. Coarse frequency measurements for the remaining data are reported in Table 3.

The current frequency history of SGR 1806–20 from year 1993 through 2000 is shown in Figure 9. As with Figure 5, the symbols mark individual frequencies and solid lines denote phase-connected timing solutions. There is no evidence for spin-up in SGR 1806–20 during the last 7.1 years. Although, as with SGR 1900+14, we note the caveat that small amplitude short-term spin-up episodes cannot be excluded due to the sparseness of the observations. The dashed line represents the average spin-down rate during the ~ 3 years prior to the 1996 burst activation of the source. At some point during late 1999, the average spin-down rate of SGR 1806–20 quadrupled

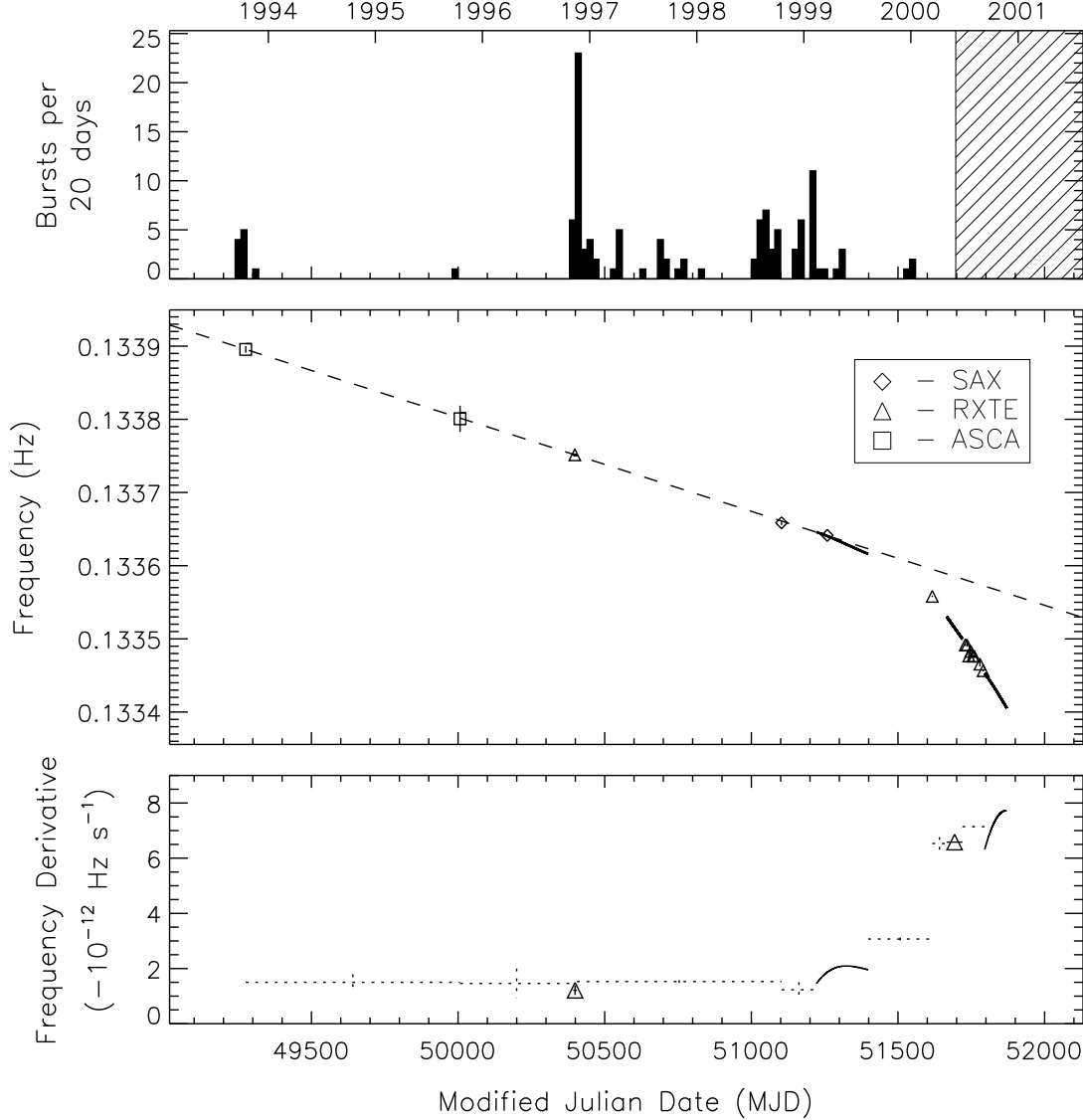


Fig. 9.— *Top* – Burst rate history of SGR 1806–20 as observed with BATSE. The hashed region starts at the end of the *CGRO* mission. *Middle* – The frequency history of SGR 1806–20 covering 7.1 years. Plotting symbols mark individual frequency measurements and solid lines denote phase-connected timing solutions. The dashed line marks the average spin-down rate prior to burst activation in 1998. *Bottom* – The frequency derivative history over the same timespan. Dotted lines denote average frequency derivative levels between widely spaced frequency measurements. Solid lines mark phase-coherent timing solutions and triangles mark instantaneous torque measurements, both using *RXTE* PCA data.

and has not yet returned to the pre-1999 rate.

The burst rate history of SGR 1806–20 as observed with BATSE is shown in the top panel of Figure 9. BATSE monitored the burst activity through the large increase in average torque in late 1999, but detected nothing out of the ordinary. As with SGR 1900+14, this interval of accelerated spin-down does not correspond to a period of strong burst activity in the SGR, but rather follows a moderate one. There is no apparent connection between the burst activity in SGR 1806–20 and the measured torque enhancement.

4. Timing Noise

Strong timing noise is present in both SGR 1806–20 and SGR 1900+14. There are numerous ways with which to characterize timing noise in pulsars. Here, we have chosen to quantify the timing noise levels in these SGRs using two separate methods in order to make comparisons to samples of both accreting systems and canonical radio pulsars. First, for each SGR, we obtain an instantaneous estimate of the timing noise parameter Δ (Arzoumanian et al. 1994). Next, using the complete frequency history, we generate torque noise power density spectra for each source (Deeter & Boynton 1982).

4.1. Δ Parameter

The timing noise parameter, Δ , is defined as $\Delta_t = \log(\frac{|\ddot{\nu}|t^3}{6\nu})$. This characterization of timing noise was introduced by Arzoumanian et al. (1994) for radio pulsars and later applied to a subset of the AXP population by Heyl & Hernquist (1999). For the radio pulsar data analyzed by Arzoumanian et al., the average timespan of the observations for each source in the sample was a few years or $\sim 10^8$ s. Therefore, Δ_8 was measured for each radio pulsar. Earlier, we calculated Δ_8 for SGR 1806–20 using a 178 day interval ($\sim 10^7$ s) of phase connected data where we could directly measure $\ddot{\nu}$ (Woods et al. 2000).

For SGR 1900+14, the longest stretch of phase connected data is 210 days in the year 2000. As was done for SGR 1806–20, we measured the average $\ddot{\nu}$ over the full extent of the data and calculated Δ_8 . We measure $\Delta_8 = 5.3$, very similar to that found for SGR 1806–20 ($\Delta_8 = 4.8$ [Woods et al. 2000]).

The Δ_8 values measured for these SGRs by far exceed any of those in the large sample of radio pulsars. Arzoumanian et al. (1994) noted that the strength of the timing noise parameter correlates with the period derivative. The two parameters scale approximately according to $\Delta_8 = 6.6 + 0.6 \log(\dot{P})$, albeit with considerable scatter about this trend. Having average period derivative values $\dot{P} \sim 10^{-10}$ s s $^{-1}$, the observed Δ_8 values of these SGRs are considerably higher than the trend (difference ~ 4.4), whereas 97% of the measured radio pulsars in the Arzoumanian

et al. sample fall within ± 1.5 in Δ_8 about the trend. Having estimated Δ_8 for some of the quieter accreting sources (Woods et al. 2000) using extended sequences of phase connected data (Chakrabarty 1996), we find that these two SGRs are “quieter” than the majority of accreting sources, yet within the range of observed timing noise strengths. Using the Δ_8 parameterization, we conclude that the timing noise in these SGRs is more in line with the accreting sources. However, Δ_8 is a relatively crude parameterization of timing noise. Given the longer temporal baseline now available to us for each SGR, we can construct meaningful torque noise power spectra which will allow us to make more detailed comparisons with accreting systems and radio pulsars.

4.2. Torque Noise Power Spectra

For each SGR, we constructed torque noise power density spectra following Deeter (1984). This technique was developed to construct power spectra for unevenly sampled data sets with non-uniform errors and is therefore very suitable for application to our SGR data. The method utilizes polynomials instead of sinusoids to estimate the power of torque fluctuations at a given analysis frequency. For the lower analysis frequencies ($\lesssim 10^{-7.2}$ Hz), we used the spin frequency histories of each SGR and fit cubic polynomial estimators. The higher analysis frequencies ($\gtrsim 10^{-7.2}$ Hz) were probed using the long stretches of phase-connected data with quartic estimators. For a more detailed description of the methodology, see §5.4 of Bildsten et al. (1997).

The SGR torque noise power spectra are extremely red and are consistent with a steep power-law. We fit these power spectra to a power-law with $\log(S_\nu) = \alpha_{7.5} + \beta \log(f_s)$, where S_ν is the power density of the frequency derivative, f_s is the analysis frequency, $\alpha_{7.5}$ is the normalization at $10^{-7.5}$ Hz, and β is the power-law index. However, a simple least squares fit to the power estimates is inadequate to accurately measure these quantities and their errors. The principle difficulties in fitting the power spectra is that each point is correlated with the others, the mid-response frequency calculated for each power measurement is dependent upon the power-law index, the errors on the power levels are only approximations within this methodology, and these errors are highly asymmetric.

To accurately parameterize the power spectra, we set up Monte Carlo simulations for each SGR data set. Only power estimates significantly above the measurement noise level ($\gtrsim 10^{-6.9}$ Hz) were utilized for this simulation. Phases and spin frequencies at each epoch were simulated according to an assumed power-law torque noise power density spectrum. One thousand realizations were constructed for a 6x6 grid of power-law normalizations and slopes with ranges which encompassed the measured values from the raw power spectra. Comparing the measured powers from the simulated data with the values input into the simulation, we found that there is a slight bias toward lower powers at the lower analysis frequencies for the SGR data (i.e. the true power is underestimated). We searched the grid for the average measured power-law parameters from the simulation which most closely agreed with those measured from the SGR data. We used the results of this simulation to remove the bias from the power measurements and to estimate the

errors on the individual powers and the measured power-law normalization and slope.

Power-law fits to the corrected SGR data yield normalizations ($\alpha_{7.5}$) of -16.36 ± 0.22 and $-17.34 \pm 0.40 \log(\text{Hz}^2 \text{ s}^{-2} \text{ Hz}^{-1})$ and power-law indices (β) of -3.7 ± 0.6 and -3.6 ± 0.7 for SGR 1900+14 and SGR 1806–20, respectively.

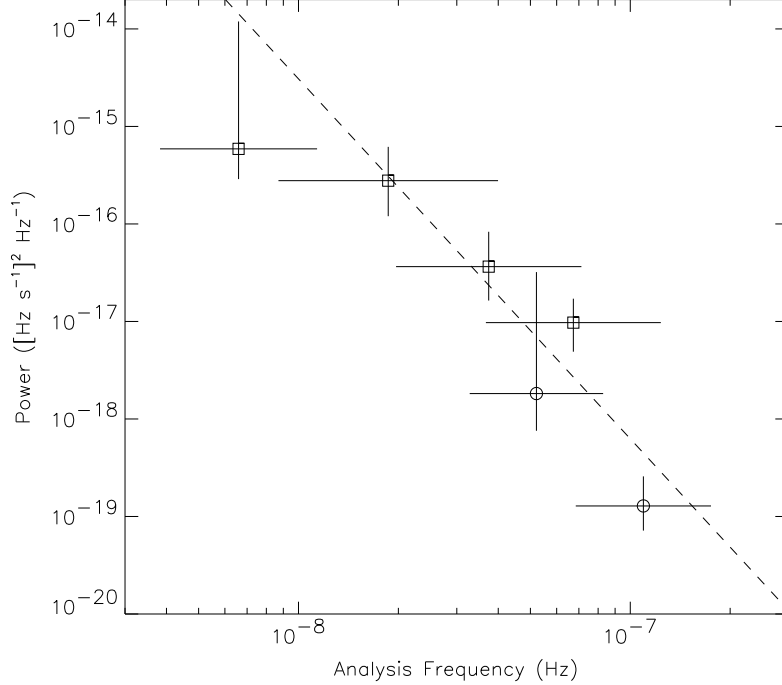


Fig. 10.— Torque noise power density spectrum of SGR 1900+14. The squares and circles denote measurements made with the frequency and phase-connected data, respectively. The data shown here have been corrected for biases introduced by the analysis method (see text for details). The errors on the power estimates denote the 68% confidence intervals which were derived from the Monte Carlo simulation. The horizontal bars give the log frequency rms of the estimator response. The power levels expected from measurement noise are much lower than the power measured from the source variability. The dashed line denotes the best power-law fit to the data.

We next compared the SGR power spectra to those of known accreting sources. Bildsten et al. (1997) noted that, in general, the wind-fed pulsars had flat power spectra and disk-fed pulsars obeyed a f^{-1} power-law. None of the measured power spectra in their sample are steeper than $\sim f^{-1.2}$. We find that the average level of the SGR torque noise power spectra are within the range of the average power for accreting systems, consistent with the Δ_8 parameterization. *However, the spectral slopes of the SGRs are much steeper than any accreting pulsar spectrum.*

Although far more phase-connected timing data are available for radio pulsars, the sample of

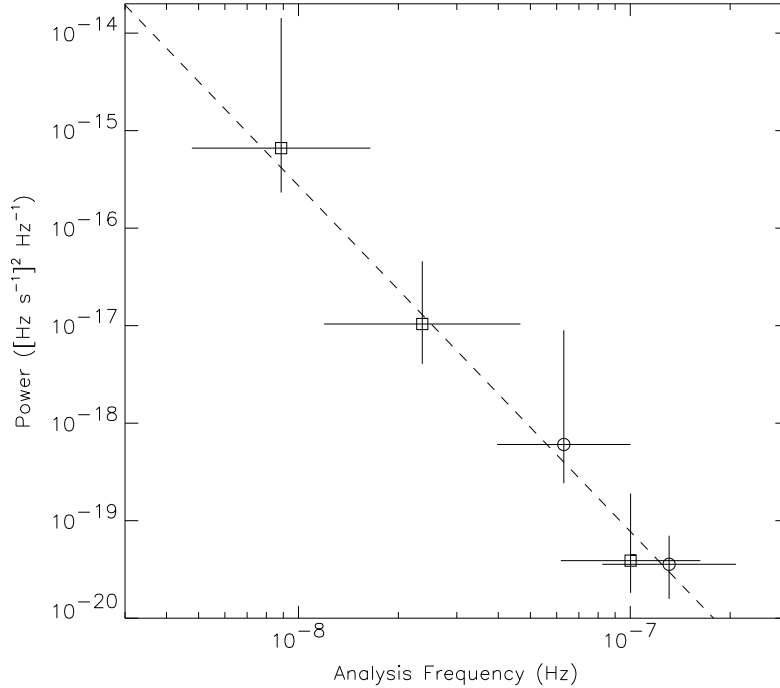


Fig. 11.— Torque noise power density spectrum of SGR 1806–20. The squares and circles denote measurements made with the frequency and phase-connected data, respectively. The data shown here have been corrected for biases introduced by the analysis method (see text for details). The errors on the power estimates denote the 68% confidence intervals which were derived from the Monte Carlo simulation. The horizontal bars give the log frequency rms of the estimator response. The power levels expected from measurement noise are much lower than the power measured from the source variability. The dashed line denotes the best power-law fit to the data.

published torque noise power spectra is very limited. From the available data, it is clear that the power spectra of radio pulsars are much more diverse than accreting pulsar power spectra. The power-law indices vary from somewhat positive values (i.e. blue spectra) to very steep negative values in some cases. For example, the Vela pulsar has a very red power spectrum, similar to the SGR power spectra. From Figure 8 of Alpar et al. (1986), we estimate $\alpha_{7.5} \approx -20.6$ and $\beta \approx -2.7$ for the Vela pulsar. Note that the power density spectrum normalization and units in Alpar et al. differ from our normalization and units by a factor $\frac{2}{(2\pi)^2}$. The factor 2 comes from our excluding power from negative frequencies and the $(2\pi)^2$ follows from the units conversion (i.e. rad s^{-1} to Hz). A complete, systematic analysis of radio pulsar data is required, however, before one can determine where the SGR torque noise power density spectra fit relative to the radio pulsar population as a whole.

5. Discussion

We have shown that the spin-down behaviors of SGR 1900+14 and SGR 1806–20 are quite erratic, and yet extremely similar to one another. The time scale of the torque variations in these SGRs varies from minutes to years and the torque noise power density spectra of these SGRs are consistent with one another in both normalization and slope. The observed range in torque imparted upon these SGRs varies by up to a factor of ~ 4 in each case despite gross differences in the burst activity of the two sources over the same time period.

There is no evidence for a direct connection between the burst activity and torque enhancements in these sources. For example, the most intense burst active interval for SGR 1900+14 was 1998 August – September, during which the spin-down rate was the lowest measured thus far. Within the first half of 2000, the spin-down rate of SGR 1900+14 was at its highest (more than four times the rate in the fall of 1998), yet there was no detectable burst emission during this entire interval. Similar examples, although less extreme, are present in the data for SGR 1806–20.

Here, we explore the hypothesis that the burst activity and torque variability may still be related, albeit with a substantial time delay between the two. The strongest torque variability observed in these SGRs thus far has been found *following* substantial burst activity. In the case of SGR 1900+14, the delay would have to be several months; for SGR 1806–20, years. While the spin frequency of SGR 1900+14 has been monitored (1996 – 2001), the source underwent relatively short intervals of concentrated burst activity including a giant flare (e.g. Hurley et al. 1999a), hard burst emission (Woods et al. 1999c), anomalously long, smooth bursts (Ibrahim et al. 2001), and multi-episodic bursts (e.g. Hurley et al. 1999c). For SGR 1806–20, the burst activity between 1996 and 2000 was more persistent and scattered in time. In spite of the large differences in burst active states between the two sources, the relative change in their spin-down rates were nearly the same. Given that the delays between burst activity and torque changes are so different between these sources and there exists no scaling of the relative change in their spin-down rates for varying degrees of burst activity, we conclude that there is no causal relationship between the burst activity and the long-term torque variability.

However, when one considers the AXP and SGR populations as a whole, the burst activity and torque variability may be linked indirectly through some other parameter (e.g. magnetic field strength). For the SGRs and AXPs, there appears to be a trend of increasing noise strength with spin-down rate (Woods et al. 2000; Gavril & Kaspi 2002), analogous to the correlation observed in radio pulsars (Cordes & Helfand 1980; Arzoumanian et al. 1994). Gavril & Kaspi (2002) suggest that this trend may represent a common bond between all three populations where the magnitude of the timing noise scales with perhaps magnetic field strength. Only sources with the strongest timing noise and largest spin-down rates (i.e. magnetic fields), namely the SGRs, have been observed to burst. Therefore, a timing noise/spin-down rate threshold in this proposed continuum may exist, above which the source will be burst active. The proximity of 1E 1048.1–5937 to the

SGRs in both spin-down rate and timing noise has led Kaspi et al. (2001) to propose that this source as the most likely candidate to undergo an ‘SGR-like’ outburst in the future.

Our monitoring of the spin behavior of these two SGRs both in burst active states as well as during quiescence enables us to constrain physical mechanisms proposed to explain, within the context of the magnetar model, the deviations from constant spin-down observed in SGRs and AXPs. It has been argued that a transient outward surface flux of Alfvén waves and particles due presumably to crust fractures associated with bursts could impart an appreciable change in torque on a magnetar (Thompson & Blaes 1998; Harding, Contopoulos & Kazanas 1999; Thompson et al. 2000). In fact, such an effect was likely detected (Woods et al. 1999b; Palmer 2001) following the extremely luminous flare of 27 August 1998 from SGR 1900+14. However, the more common, shorter bursts have shown no evidence for associated transient torque changes. The difference in energy between the giant flare and the recurrent bursts is several orders of magnitude ($\gtrsim 3$) and the predicted energy dependence of the stellar angular momentum change goes as E (Thompson et al. 2000). Considering the energy difference and the short timescale over which the transient 27 August torque change acted (Palmer 2001), it is not surprising that the other burst activity from SGR 1900+14 and all observed activity from SGR 1806–20 have had no measurable effect on the spin-down of their respective SGRs.

The absence of a direct correlation between burst activity and torque enhancements has strong implications for the underlying physics behind each phenomenon. The magnetar model postulates that the bursting activity in SGRs is a result of fracturing of the outer crust of a highly magnetized neutron star (Thompson & Duncan 1995). Furthermore, the majority of models proposed to explain the torque variability in magnetars invoke crustal motion and/or low-level seismic activity (e.g. Thompson et al. 2000). Since we have found no direct correlation between the burst activity and torque variability, we conclude that either (*i*) the seismic activities leading to each observable are decoupled from one another, or (*ii*) at least one of these phenomena is *not* related to seismic activity.

Precession models, both radiative (Melatos 1999) and free (Thompson et al. 2000), were proposed previously as possible explanations for the observed variability in spin-down in SGRs and AXPs. These models predict periodic variations in the spin-down on timescales of several months to several years. It is clear from the present data that periodic torque variations on short timescales (i.e. less than a few years) can be excluded. Given the relatively short baseline of the spin frequency histories for these SGRs, one cannot rule out precessional periods longer than a few years, although, the strong, short-term variations must still be explained through some other process.

6. Conclusions

Using predominantly *RXTE* PCA observations, we have constructed long-term frequency histories for SGR 1900+14 and SGR 1806–20. Each SGR exhibits large excursions from constant spin-down although neither has shown evidence for spin-up. The torque variability does not correlate with the burst activity in either source, contrary to predictions from some models. The absence of a correlation between burst activity and torque variability places significant constraints on the physical mechanisms behind each phenomenon in the context of the magnetar model. Specifically, either the seismic activities leading to the burst activity and torque variability are physically decoupled from one another or at least one of these phenomena are not related to seismic activity.

Using phase-connected timing solutions and the global frequency histories, we construct torque noise power density spectra for each SGR. The torque noise power spectra are consistent with one another, but do not match the power spectra of accreting systems or standard radio pulsars. The SGR torque noise spectra are much steeper than power spectra of accreting systems and the frequency averaged power levels are much higher than the spectra of radio pulsars. Construction and modeling of torque noise power density spectra for AXPs and a large collection of radio pulsars would provide a useful quantitative means for comparison of timing noise behavior between these three classes of neutron stars.

Acknowledgements – We greatly appreciate the help we received from the *RXTE* team, particularly Evan Smith and the SOF for scheduling these extensive observations. We also thank the *RXTE*/SDC, the *SAX*/SDC, and HEASARC for pre-processing the *RXTE*/PCA and BeppoSAX data. This work was funded primarily through a Long Term Space Astrophysics program (NAG 5-9350) for both PMW and CK. MHF and EG acknowledge support from the cooperative agreement NCC 8-200. PMW, CK, and EG appreciate useful discussions at the ITP funded by NSF grant PHY99-07949.

REFERENCES

- Alpar, M.A., Nandkumar, R. & Pines, D. 1986, *ApJ*, 311, 197
- Arzoumanian, Z., Nice, D.J., Taylor, J.H. & Thorsett, S.E. 1994, *ApJ*, 422, 671
- Bildsten, L., et al. 1997, *ApJS*, 113, 367
- Boynton, P.E., Groth, E.J., Hutchinson, D.P., Nanos, G.P., Partridge, R.B. & Wilkinson, D.T. 1972, *ApJ*, 175, 217
- Chakrabarty, D. 1996, PhD Thesis, Cal Tech
- Cordes, J.M. & Helfand, D.J. 1980, *ApJ*, 239, 640
- Deeter, J.E. & Boynton P.E. 1982, *ApJ*, 261, 337
- Deeter, J.E. 1984, *ApJ*, 281, 482
- Duncan, R. & Thompson, C. 1992, *ApJ*, 392, L9
- Frail, D., Kulkarni, S. & Bloom, J. 1999, *Nature*, 398, 127
- Feroci, M., Frontera, F., Costa, E., Amati, L., Tavani, M., Rapisarda, M., & Orlandini, M. 1999, *ApJ*, 515, L9
- Feroci, M., Hurley, K., Duncan, R.C. & Thompson, C. 2001, *ApJ*, 549, 1021
- Gavriil, F. & Kaspi, V.M. 2002, *ApJ*, 567, 1067
- Göğüş, E., Kouveliotou, C., Woods, P.M., Thompson, C., Duncan, R.C., & Briggs, M.S. 2001, *ApJ*, 558, 228
- Gold, T. 1968, *Nature*, 218, 731
- Harding, A.K., Contopoulos, I., & Kazanas, D. 1999, *ApJ*, 525, L125
- Hewish, A., Bell, S.G., Pilkington, J.D.H., Scott, P.F., Collins, R.A. 1968, *Nature*, 217, 709
- Heyl, J.S. & Hernquist, L. 1999, *MNRAS*, 304, L37
- Hulleman, F., van Kerkwijk, M.H. & Kulkarni, S.R. 2000, *Nature*, 408, 689
- Hulleman, F., van Kerkwijk, M.H., Verbunt, F.W.M. & Kulkarni, S.R. 2000, *A&A*, 358, 605
- Hurley, K., et al. 1999a, *Nature*, 397, 41
- Hurley, K., et al. 1999b, *ApJ*, 510, L111
- Hurley, K., Kouveliotou, C., Woods, P., Cline, T., Butterworth, P., Mazets, E., Golenetskii, S. & Frederiks, D. 1999c, *ApJ*, 510, L107
- Hurley, K. 2000, in *AIP Conf. Proc.* 526, *Gamma-Ray Bursts: 5th Huntsville Symp.*, ed. R.M. Kippen, R.S. Mallozzi, & G.J. Fishman, (New York:AIP), 763
- Ibrahim, A., Strohmayer, T.E., Woods, P.M., Kouveliotou, C., Thompson, C., Duncan, R.C., Dieters, S., van Paradijs, J. & Finger M. 2001, *ApJ*, 558, 237
- Ioka, K. 2001, *MNRAS*, 327, 639

- Kaplan, D.L., Kulkarni, S.R., van Kerkwijk, M.H., Rothschild, R.E., Lingenfelter, R.L., Marsden, D., Danner, R. & Murakami, T. 2001, *ApJ*, 556, 399
- Kaspi, V.M., Gavril, F.P., Chakrabarty, D., Lackey, J.R. & Muno, M.P. 2001, *ApJ*, 558, 253
- Kern, B. & Martin, C. 2001, *IAU Circ.* 7769
- Kouveliotou, C., et al. 1998, *Nature*, 393, 235
- Kouveliotou, C., et al. 1999, *ApJ*, 510, L115
- Kouveliotou, C., et al. 2001, *ApJ*, 558, L47
- Lomb, N.R. 1976, *Astro. & Space Sci.*, 39, 447
- Marsden, D., Rothschild, R.E., & Lingenfelter, R.E. 1999, *ApJ*, 523, L97
- Mazets, E.P., Golenetskii, S.V., Il'inskii, V.N., Aptekar, R.L. & Guryan, Yu. A. 1979, *Nature*, 282, 587
- Mazets, E.P., Cline, T., Aptekar, R.L., Butterworth, P., Frederiks, D.D., Golenetskii, S.V., Il'inskii, V.N., & Pal'shin, V.D. 1999, *Astron. Lett.*, 25, 635
- Melatos, A. 1999, *ApJ*, 519, L77
- Mereghetti, S., Israel, G.L. & Stella, L. 1998, *MNRAS*, 296, 689
- Mereghetti, S. 2000, in *NATO Science Series Vol. 567, The Neutron Star – Black Hole Connection*, ed. C. Kouveliotou, J. Ventura, & E. van den Heuvel, (The Netherlands:Kluwer), 351
- Özel, F. 2001, *ApJ*, 563, 276
- Özel, F., Psaltis, D. & Kaspi, V.M. 2001, *ApJ*, 563, 255
- Pacini, F. 1967, *Nature*, 216, 567
- Paczynski, B. 1992, *Acta Astron.*, 42, 145
- Palmer, D.M. 2001, in *Soft Gamma Repeaters: The Rome 2001 Mini-Workshop*, astro-ph/0103404
- Patel, S.K., Kouveliotou, C., Woods, P.M., Tennant, A.F., Weisskopf, M.C., Finger, M.H., Göğüş, E., van der Klis, M. & Belloni, T. 2001, *ApJ*, 563, L45
- Radhakrishnan, V. & Manchester, R.M. 1969, *Nature*, 222, 228
- Reichley, P.E. & Downs, G.S. 1969, *Nature*, 222, 229
- Richards, D.W. & Comella, J.M. 1969, *Nature*, 222, 551
- Thompson, C., & Blaes, O. 1998, *Phys. Rev. D*, 57, 3219
- Thompson, C., & Duncan, R. 1995, *MNRAS*, 275, 255
- Thompson, C., & Duncan, R. 1996, *ApJ*, 473, 322
- Thompson, C., Duncan, R., Woods, P.M., Kouveliotou, C., Finger, M.H., & van Paradijs, J. 2000, *ApJ*, 543, 340
- Wilson, C.A., Dieters, S., Finger, M.H., Scott, D.M. & van Paradijs, J. 1999, *ApJ*, 513, 464

Woods, P.M., Kouveliotou, C., van Paradijs, J., Finger, M.H., & Thompson, C. 1999a, ApJ, 518, L103

Woods, P.M., et al. 1999b, ApJ, 524, L55

Woods, P.M., et al. 1999c, ApJ, 527, L47

Woods, P.M., et al. 2000, ApJ, 535, L55

Woods, P.M., et al. 2001, ApJ, 552, 748

Table 1: Pulse frequencies for SGR 1900+14.

Date mm/dd/yy	MJD TDB	Frequency (Hz)
01/03/99	51181.590	0.19376364(23)
01/05/99	51183.210	0.1937596(28)
01/09/99	51187.274	0.193760(4)
01/17/99	51195.073	0.193753(4)
01/25/99	51203.069	0.193762(6)
02/01/99	51210.940	0.193759(5)
02/09/99	51218.158	0.1937475(28)
02/17/99	51226.992	0.193750(4)
02/25/99	51234.055	0.193744(10)
03/05/99	51242.178	0.193744(7)
03/13/99	51250.882	0.193741(12)
03/21/99	51258.782	0.193733(9)
03/31/99	51268.009	0.193740(5)
04/06/99	51274.870	0.193735(9)
04/14/99	51282.969	0.1937307(27)
04/23/99	51291.794	0.193726(9)
05/01/99	51299.691	0.193759(13)
05/09/99	51307.883	0.193723(7)
05/17/99	51315.882	0.19372(7)
05/25/99	51323.848	0.193724(5)
06/02/99	51331.865	0.193720(17)
06/18/99	51347.427	0.193710(9)
06/25/99	51354.920	0.193733(10)
07/02/99	51361.640	0.193730(11)
07/12/99	51371.693	0.193699(13)
07/19/99	51378.172	0.193697(14)
07/27/99	51386.918	0.193690(6)
03/30/00 ^a	51633.500	0.1935327(9)
04/26/00 ^a	51660.000	0.1935115(10)

a – *BeppoSAX* observation: all others use *RXTE* PCA data

Table 2: Year 2000 pulse ephemeris for SGR 1900+14 from *RXTE* PCA observations.

Parameter	Ephemeris 2000
Date Range	2000 June 09 – 2001 January 04
MJD Range	51704.2 – 51914.9
Epoch (MJD)	51780.0
χ^2/dof	23.3/20
ν (Hz)	0.193464095(8)
$\dot{\nu}$ (10^{-12} Hz s $^{-1}$)	-2.913(3)
$\ddot{\nu}$ (10^{-19} Hz s $^{-2}$)	-1.72(3)
$\nu^{(3)}$ (10^{-26} Hz s $^{-3}$)	-1.21(8)
$\nu^{(4)}$ (10^{-32} Hz s $^{-4}$)	1.33(9)
$\nu^{(5)}$ (10^{-39} Hz s $^{-5}$)	-4.7(4)

Table 3: Pulse frequencies for SGR 1806–20 from *RXTE* PCA observations.

Date	MJD	Frequency
mm/dd/yy	TDB	(Hz)
03/14/00	51617.000	0.1335581(10)
07/04/00	51729.844	0.1334919(16)
07/10/00	51735.519	0.1334915(22)
07/16/00	51741.478	0.133477(6)
07/23/00	51748.413	0.1334830(12)
07/30/00	51755.496	0.1334765(13)
08/04/00	51760.321	0.1334764(23)
08/12/00	51768.801	0.133454(21)
08/23/00	51779.522	0.1334655(33)
09/03/00	51790.574	0.1334566(10)

Table 4: Year 2000 pulse ephemerides for SGR 1806–20 from *RXTE* PCA observations.

Parameter	Ephemeris 2000a	Ephemeris 2000b
Date Range	2000 May 01 – June 24	2000 September 08 – November 23
MJD Range	51666.0 – 51719.9	51795.8 – 51871.6
Epoch (MJD)	51690.0	51840.0
χ^2/dof	6.7/5	11.0/7
ν (Hz)	0.133516758(7)	0.13342617(2)
$\dot{\nu}$ (10^{-12} Hz s $^{-1}$)	-6.58(1)	-7.516(22)
$\ddot{\nu}$ (10^{-20} Hz s $^{-2}$)	...	-1.78(21)
$\nu^{(3)}$ (10^{-26} Hz s $^{-3}$)	...	8.0(28)